



# Corrosion Inhibition by Self-assembling Nano films of Tween 60 on Mild steel surface

V.R.Nazeera Banu, S.Rajendran, S.S.Syed Abuthahir

Department of Chemistry, RVS College of Engineering, Dindigul, Tamilnadu, India.

Department of Chemistry, RVS School of Engineering and Technology, Dindigul, Tamilnadu, India.

Department of Chemistry, Jamal Mohammed College, Trichy, Tamilnadu, India.

**Abstract :** The surface of mild steel was modified by the formation of Tween 60 Self-assembling nano films to increase the corrosion inhibition ability. Formation of Self-assembled nano films takes place when mild steel is immersed in well water in presence of 200 ppm of Tween 60 and 50 ppm of  $Zn^{2+}$  for one day, shows 88 % corrosion inhibition efficiency. The modified surface was characterized by polarization, cyclic voltammetry, FT-IR spectroscopy, SEM and EDS micrographs. Atomic Force Microscopy confirmed the formation of lesser amounts of corrosion products on the Self-assembling nano film protected surface. The nano film is found to be hydrophobic in nature. This is confirmed by contact angle measurement.

**Keywords** Tween 60, Polarization, SEM, AFM, Contact angle measurement

## Introduction

Mild steel is one of the least expensive and most widely investigated engineering alloys for corrosion inhibition studies. One of the choices to reduce the corrosion of steel to safe limits is the use of inhibitors<sup>1,2</sup>. Corrosion Inhibitors, which work at the interface of the corrosive media and the metal surface, hinder the corrosion rate of the metal when present in the corrosive media at a suitable concentration. Most of the organic compounds used as inhibitor are synthetic chemicals, expensive, and very hazardous to both human beings and the environments and need to be replaced with cheap, non-toxic and eco-friendly compounds<sup>3,4,5,6,7,8</sup>. Now a days, surfactants have been identified to be attractive as corrosion inhibitors as they are cost effective. They are inherently stable and non-toxic and exhibit greater corrosion inhibition properties in contrast to simple organic molecules. Surfactants have been used as corrosion inhibitors by a number of investigators<sup>9,10,11</sup>. The surfactants through their active site form complexes with metal ions and there is a formation of self-assembling nano films on the metal surface<sup>12</sup>, thus, covering the surface and protecting the metal from corrosion. In this work, we have evaluated the corrosion inhibition properties of Tween 60 self-assembling nano films on mild steel.

The present work is undertaken (i) to evaluate the inhibition efficiency of Tween 60 SAMs for the corrosion of mild steel (ii) to analyze the protective film on mild steel by FTIR spectra (iii) to know the mechanistic aspects of corrosion inhibition by potentiodynamic polarization studies (iv) to study the hydrophobization of the Tween 60 nano films by contact angle measurements. (v) to propose a suitable mechanism for corrosion inhibition.

## Experimental

The chemicals used in this study, Tween 60 inhibitor and  $\text{ZnSO}_4 \cdot 7\text{H}_2\text{O}$  ( $\text{Zn}^{2+}$  ions) co inhibitor were AR grade.

### Preparation of the specimen

Mild steel specimens of dimensions 1.0 cm X 4.0 cm X 0.2 cm (are 10 cm<sup>2</sup>) and chemical composition Sulphur 0.026 %, Manganese 0.4 %, Phosphorous 0.06 %, Carbon 0.1 % and the rest iron, were polished to a mirror finish and degreased with trichloroethylene.

### Mass-loss Method

Mild steel specimens in triplicate were immersed in 100 mL of the well water medium containing different concentrations of the inhibitor (Tween 60) in the absence and presence of  $\text{Zn}^{2+}$  for one day. The weight of the specimens before and after immersion were determined using Shimadzu Ay 62 model. The inhibition efficiency (IE) was calculated using the equation (1)

$$\text{IE} = 100 [1 - W_2/W_1] \% \quad (1)$$

Where,  $W_1$  is the weight loss value in the absence of inhibitor and  $W_2$  is the weight loss value in the presence of inhibitor.

### Surface examination study

The mild steel specimens were immersed in different test solutions for a period of one day. After exposure, the specimens were removed and dried. The nature of the film formed on the surface of the metal specimens was analyzed by various surface analysis techniques.

### Potentiodynamic polarization study

Potentiodynamic polarization studies were carried out by CHI electrochemical impedance analyzer, model 660A. A three-electrode cell assembly was employed. The working electrode was mild steel. A saturated calomel electrode (SCE) was used as the reference electrode and a rectangular platinum foil was used as the counter electrode (Figure 1).

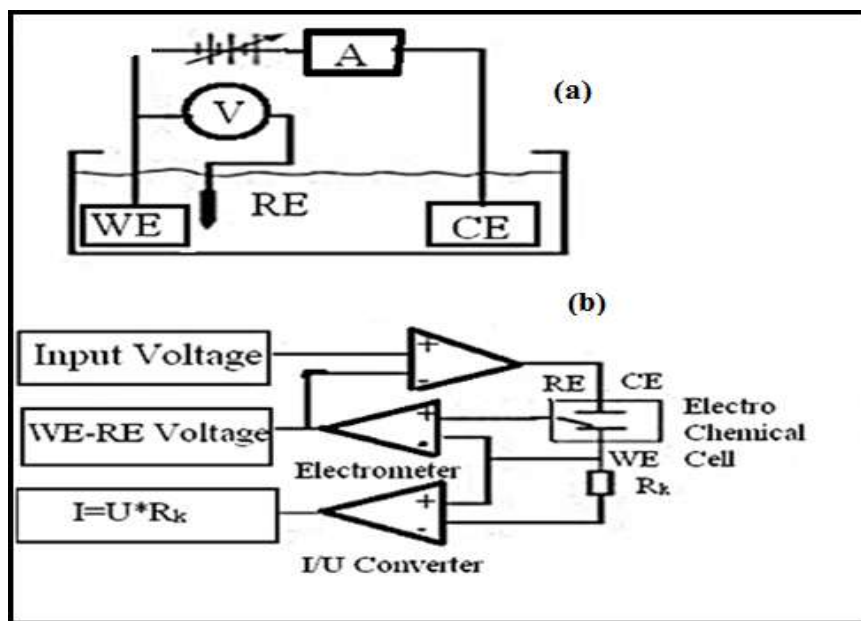


Figure 1 (a) Three electrode cell assembly (b) A Schematic representation of a three electrodepotentiostat.

### FT-IR spectra

The film formed on the mild steel surface was removed carefully and mixed thoroughly with KBr. The FTIR spectra were recorded by using a Perkin-Elmer 1600 FTIR spectrophotometer (KBr pellet).

### Scanning Electron Microscopic studies (SEM)

The mild steel immersed in blank solution and in the inhibitor solution for one day was removed, rinsed with double distilled water, dried and observed in a scanning electron microscope to examine the surface morphology. The surface morphology measurements of mild steel were examined using JEOL MODEL 6390 computer controlled scanning electron microscope.

### Contact angle measurements

The contact angle measurements for the mild steel surface were recorded using a VCA Optima instrument equipped with a CCD camera for imaging. The double distilled water under static conditions with a drop volume of 5 mL was used to determine the contact angle. VCA Optima XC software provided with instruments was used for fitting the drop shapes to find the contact angle of water on the mild steel surface. The contact angle measurement was repeated three times for each mild steel surface, and the average values with standard deviations  $\pm 2$  degree are reported.

### Atomic Force Microscopy Characterization (AFM)

Atomic Force Microscope (AFM) is a new technique which permits metal surface to be imaged at higher resolutions and accuracies than ever before. The mild steel specimen immersed in blank and in the inhibitor system for one day. The mild steel specimens were removed, rinsed with double distilled water, dried, and subjected to the surface examination. VeecoInnova model was used to observe the mild steel surface in tapping mode, using cantilever with linear tips. The scanning area of the images was  $50 \mu\text{m} \times 50 \mu\text{m}$  and the scan rate was  $0.6 \text{ Hz S}^{-1}$ . A two dimensional, and a three dimensional topography of mild steel surface films gave various roughness parameters of the film.

## Results and Discussions

### Analysis of Results of mass- loss study

The physicochemical parameters of well water are given in Table 1. Corrosion rates (CR) of mild steel immersed in well water in the absence and presence of inhibitor (Tween 60) are given in Tables 2 and 3. The inhibition efficiencies (IE) are also given in these Tables. The inhibition efficiencies of the Tween 60 -  $\text{Zn}^{2+}$  systems as a function of concentrations of Tween 60 are shown in Figure 2.

**Table 1. Parameters of well water**

Parameters	Value
pH	8.38
Total Dissolved Solids	2010 ppm
Magnesium	81 ppm
Nitrate	0
Chloride	661 ppm
Sulphate	11 ppm
Sodium	168 ppm
Fluoride	0
Potassium	48 ppm
Total Hardness as $\text{CaCO}_3$	1101 ppm

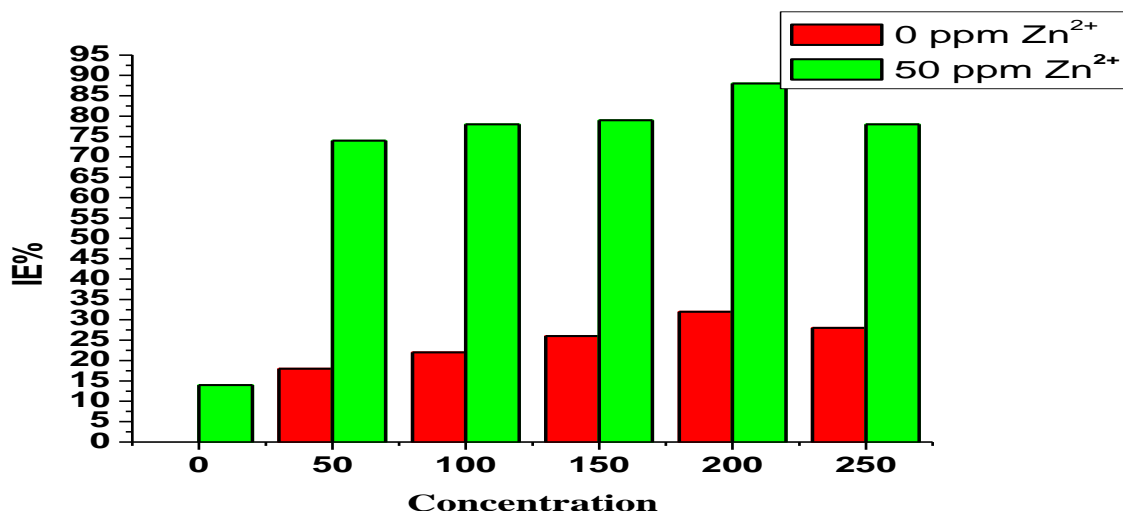


Figure 2 Inhibition efficiencies (IE) of mild steel immersed in various test solutions

Table 2. Corrosion rates (CR) of mild steel immersed in well water in the presence and absence of inhibitor system at various concentrations and the inhibition efficiencies (IE) obtained by weight loss method Tween 60 - Zn<sup>2+</sup> (0 ppm).

Tween 60 (200 ppm)	Zn <sup>2+</sup> (50 ppm)	CR (mdd)	IE%
0	0	18.18	-
50	0	14.91	18
100	0	14.18	22
150	0	13.45	26
200	0	12.36	32
250	0	13.09	28

It is observed from Table 2 that Tween 60 shows some inhibition efficiencies. 200 ppm of Tween 60 has 32 % inhibition efficiency, as the concentration of Tween 60 increases, the inhibition efficiency increases. This is due to the fact that as the concentration of Tween 60 increases, the protective film (probably Fe -Tween 60 complex) formed on the metal surface. At concentrations  $\geq 250$  ppm of Tween 60, the protection efficiency decreases. It may be due to the fact that these molecules aggregate together to form micelles. They are not uniformly adsorbed on the metal surface. Hence corrosion inhibition efficiently decreases.

#### Influence of Zn<sup>2+</sup> on the inhibition efficiencies of Tween 60

The influence of Zn<sup>2+</sup> on the inhibition efficiencies of Tween 60 is given in Table 3. It is observed that as the concentration of Tween 60 increases the IE increases. At concentrations  $\geq 250$  ppm of Tween 60, the protection efficiency decreases. It may be due to the fact that these molecules aggregate together to form micelles. They are not uniformly adsorbed on the metal surface. Hence corrosion inhibition efficiently decreases. It is also observed that a synergistic effect exists between Tween 60 and Zn<sup>2+</sup>. For example, 50 ppm of Zn<sup>2+</sup> has 18 % IE; 200 ppm of Tween 60 has 32 % IE. Interestingly their combination has a high IE, namely 88 %.

**Table 3. Corrosion rates (CR) of mild steel immersed in well water in the presence and absence of inhibitor system at various concentrations and the inhibition efficiencies (IE) obtained by weight loss method Tween 60 - Zn<sup>2+</sup> (50 ppm).**

Tween 60 (200 ppm)	Zn <sup>2+</sup> (50 ppm)	CR (mdd)	IE%
0	0	18.18	-
0	50	15.85	14
50	50	4.73	74
100	50	3.99	78
150	50	3.82	79
200	50	2.18	88
250	50	3.99	78

In the presence of Zn<sup>2+</sup> more amount of Tween 60 is transported towards the metal surface. On the metal surface Fe<sup>2+</sup>- Tween 60 complex is formed on the anodic sites of the metal surface. Thus the anodic reaction is controlled. The cathodic reaction is the generation of OH<sup>-</sup>, which is controlled by the formation of Zn(OH)<sub>2</sub> on the cathodic sites of the metal surface. Thus the anodic reaction and cathodic reaction are controlled effectively. This accounts for the synergistic effect existing between Zn<sup>2+</sup> and Tween 60.

Fe → Fe<sup>2+</sup> + 2e<sup>-</sup> (Anodic reaction)

Fe<sup>2+</sup> + Zn<sup>2+</sup>- Tween 60 complex → Fe<sup>2+</sup>- Tween 60 complex + Zn<sup>2+</sup>

O<sub>2</sub> + 2H<sub>2</sub>O + 4e<sup>-</sup> → 4OH<sup>-</sup> (Cathodic reaction)

Zn<sup>2+</sup> + 2OH<sup>-</sup> → Zn(OH)<sub>2</sub>↓

#### Analysis of potentiodynamic polarization study

Polarization study has been used to confirm the formation of protective film on the mild steel surface during corrosion inhibition process. If a protective film is formed on the mild steel surface, the linear polarization resistance value (LPR) increases and the corrosion current value (I<sub>Corr</sub>) decreases.

**Table 4. Corrosion parameters of mild steel immersed in well water in the absence and presence of inhibitor system obtained from potentiodynamic polarization study.**

System	E <sub>Corr</sub> mV Vs SCE	bc mV/ decade	ba mV/ decade	I <sub>Corr</sub> A/cm <sup>2</sup>	LPR ohmcm <sup>2</sup>
Well water	-828	6.052	6.091	8.915x10 <sup>-7</sup>	35319.7
Well water + Tween 60 (200 ppm) + Zn <sup>2+</sup> (50 ppm)	-872	6.269	6.267	7.145 x10 <sup>-7</sup>	37276.5

The potentiodynamic polarization curves of mild steel immersed in well water in the absence and presence of inhibitors are shown in Figures 3a and 3b. The corrosion parameters such as corrosion potential, corrosion current, LPR, Tafel slopes, b<sub>a</sub> and b<sub>c</sub> are given in Table 4. When mild steel was immersed in well water the corrosion potential was -828mV Vs SCE. When Tween 60 (200 ppm) and Zn<sup>2+</sup> (50 ppm) were added to the above system the corrosion potential shifted to the noble side -872 mV Vs SCE. This shows that the corrosion potential difference is very small therefore behaving like mixed type inhibitor which controls both anodic and cathodic reaction to an equal extent. This suggests that a protective film is formed on the metal surface<sup>13, 14, 15</sup>.

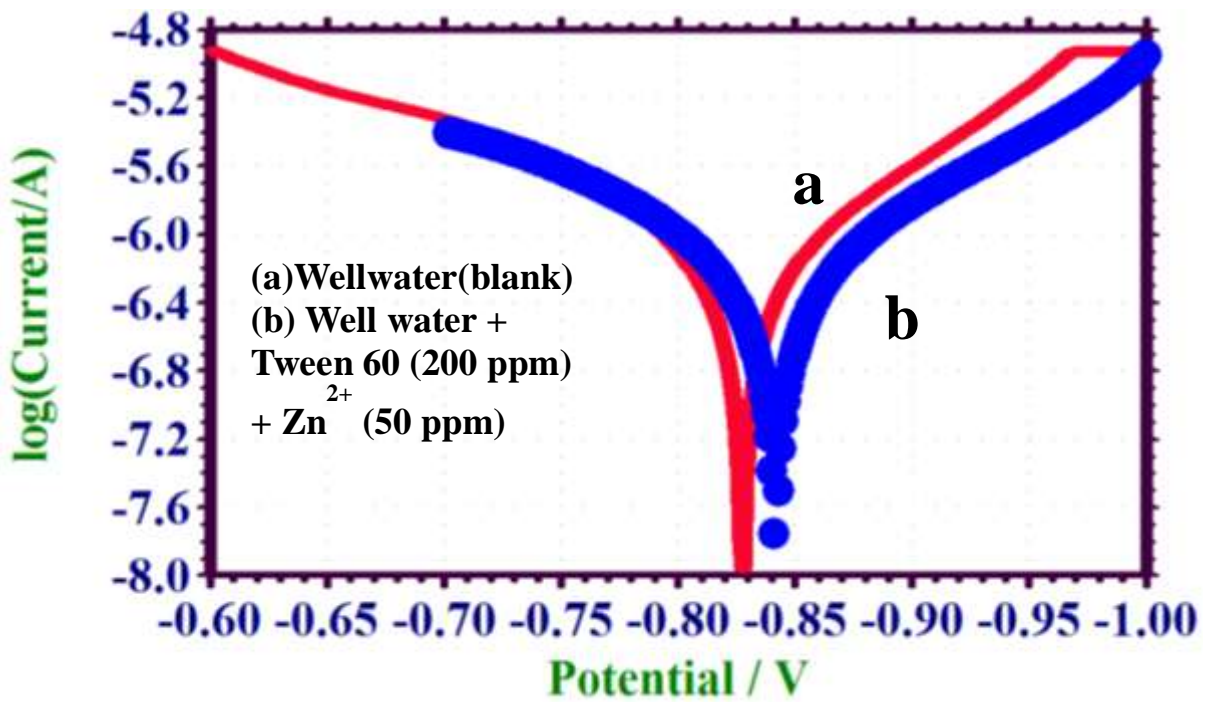
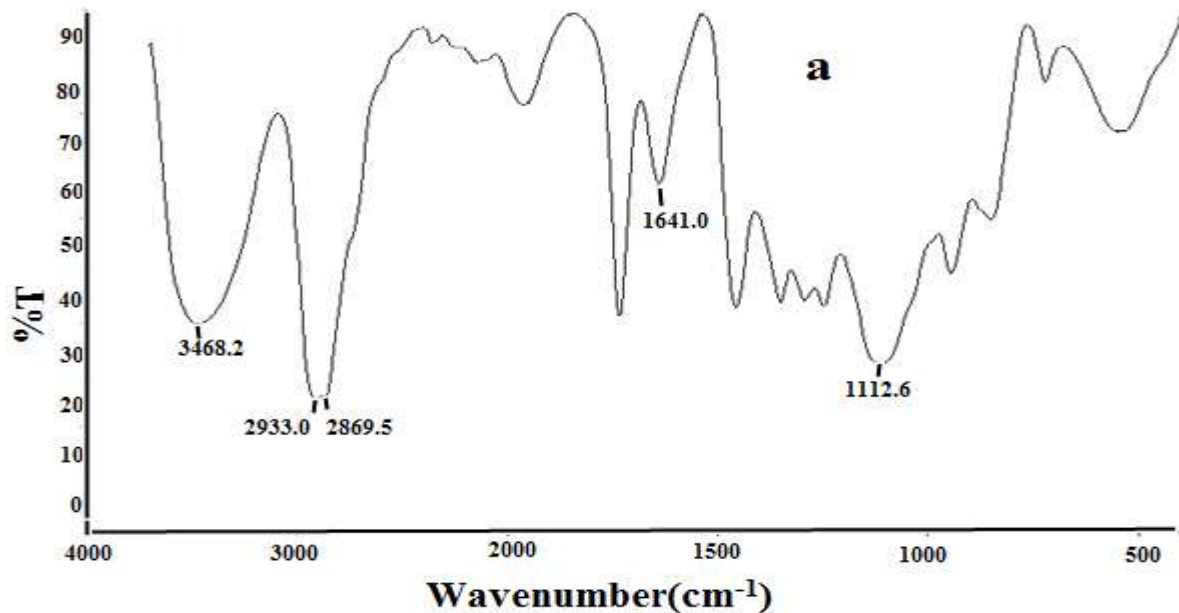


Figure 3 Polarization curves of mild steel immersed in various test solutions Well water (blank) (b) Well water + Tween 60 (200 ppm) + Zn<sup>2+</sup> (50 ppm)



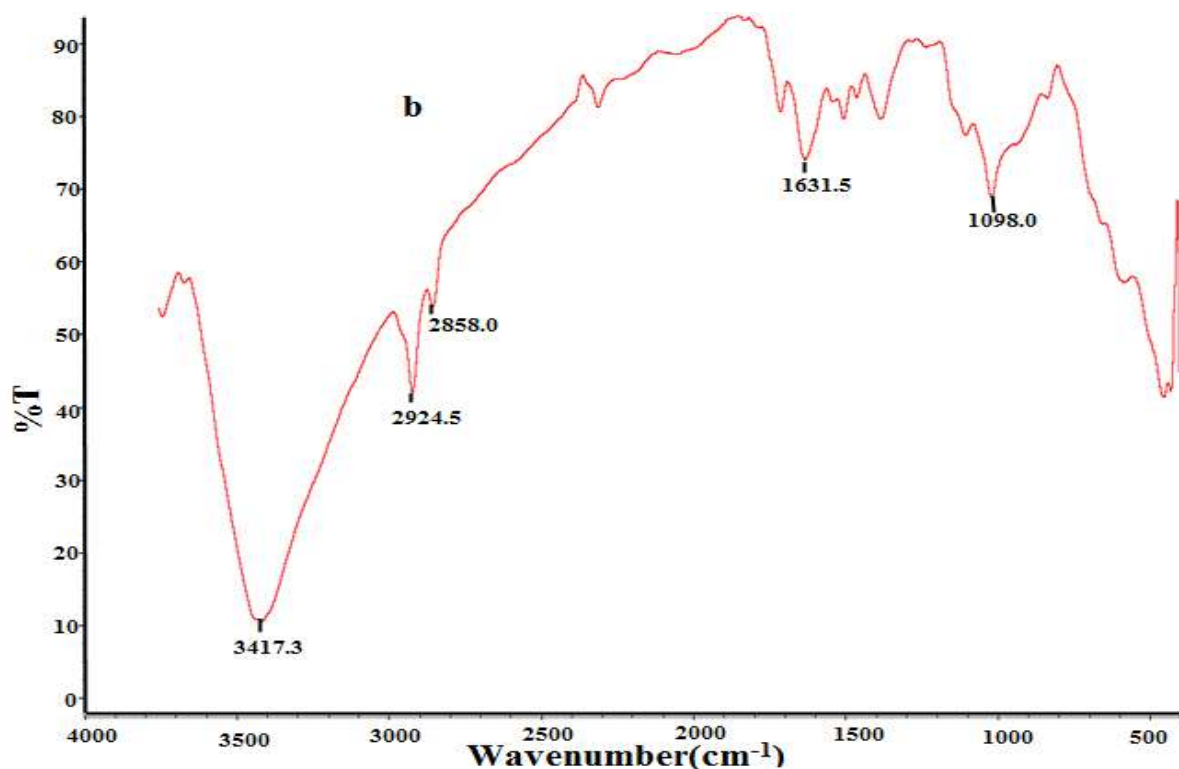


Figure 4. FTIR Spectrum of (a) Pure Tween 60 (b) Well water + Tween 60 (200 ppm) +  $Zn^{2+}$  (50 ppm)

#### Analysis of FT-IR spectra

FTIR spectra have been used to analysis the protective film formed on the metal surface<sup>16</sup>. The FTIR spectrum (KBr) of pure Tween 60 is shown in Figure 4a. The FTIR spectrum of the film formed on the metal surface after immersion in the solution containing well water, 200 ppm of Tween 60 and 50 ppm  $Zn^{2+}$  is shown in Figure 4b. The peak at  $3468\text{ cm}^{-1}$  is due to  $OH^-$  stretching shifted to  $3417\text{ cm}^{-1}$ . The C=O stretching frequency has shifted from  $1641.0\text{ cm}^{-1}$  to  $1631.5\text{ cm}^{-1}$ . This observation suggest that Tween 60 has coordinated with  $Fe^{2+}$  on metal surface through oxygen atom of resulting in the formation of  $Fe^{2+}$ - Tween 60 complex on the anodic sites of the metal surface. The spectrum exhibits a strong C-O-C band at  $1112.6\text{ cm}^{-1}$  is shifted to  $1098.0\text{ cm}^{-1}$ . The C-H stretching frequency has shifted from  $2933.0$  to  $2924.5\text{ cm}^{-1}$ . Thus the FTIR spectral study leads to the conclusion that the protective film consist of  $Fe^{2+}$ - Tween 60 and  $Zn(OH)_2$ .

#### SEM Analysis of metal surface

SEM provides a pictorial representation of the surface<sup>17, 18</sup>. To understand the nature of the metal surface film in the absence and the presence of inhibitors and the extent of corrosion of mild steel, the SEM micrographs of the surface are examined.

The SEM images of different magnifications (X1000,X2000) of mild steel specimen and mild steel specimen immersed in well water for one day in the absence and presence of inhibitor system are shown in Figure 5 as images (a,b,c,d,e and f) respectively.

The SEM micrographs of polished mild steel surface (control) in Figure 5 images (a,b) illustrate the smooth surface of the metal. These show the absence of any corrosion products formed on the metal surface.

The images (c,d) denote the SEM micrographs of mild steel surface immersed in well water. They show the type of rough surface characteristic of the uniform corrosion of the metal surface in well water, indicating in an inhibitor free solution, the surface is highly corroded.

The images (e,f) confirm that in the presence of 200 ppm Tween 60 and 50 ppm of  $Zn^{2+}$  mixture in well water, the rate of corrosion is suppressed, as can be seen from the decrease in corroded areas. This is as a result of the

formation of insoluble complex on the surface of the metal (Tween 60-Zn<sup>2+</sup> inhibitor complex) and the surface is mild steel. These results corroborate all of the electrochemical and weight loss measurements.

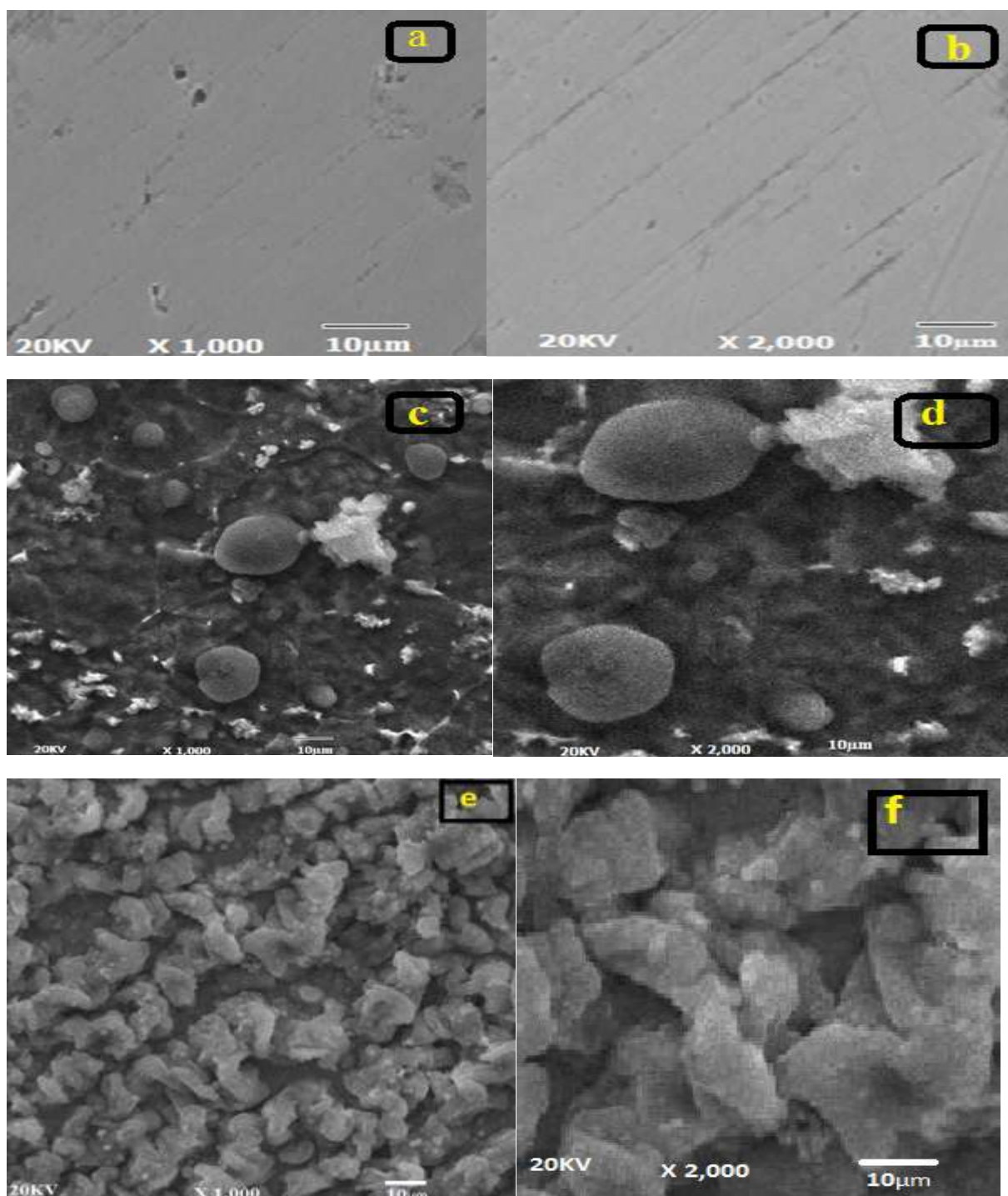


**Figure 5. Scanning Electron Micrographs of (a) Pure Tween 60 (b) Well water + Tween 60 (200 ppm) + Zn<sup>2+</sup> (50 ppm)**

#### Contact Angle measurements

Contact Angle measurement is extremely helpful to recognize the hydrophobic nature and the arrangement of Self-assembling nano films on the metal surface<sup>19, 20</sup>. When Self-assembling nano films are formed on metal surface, the surface becomes hydrophobic hence it becomes water repellent. Water molecules cannot sit on the metal surface this is very similar to lotus effect (water droplets rolling on lotus leaves) so corrosion is prevented. As the hydrophobicity increases corrosion inhibition nature also increases.

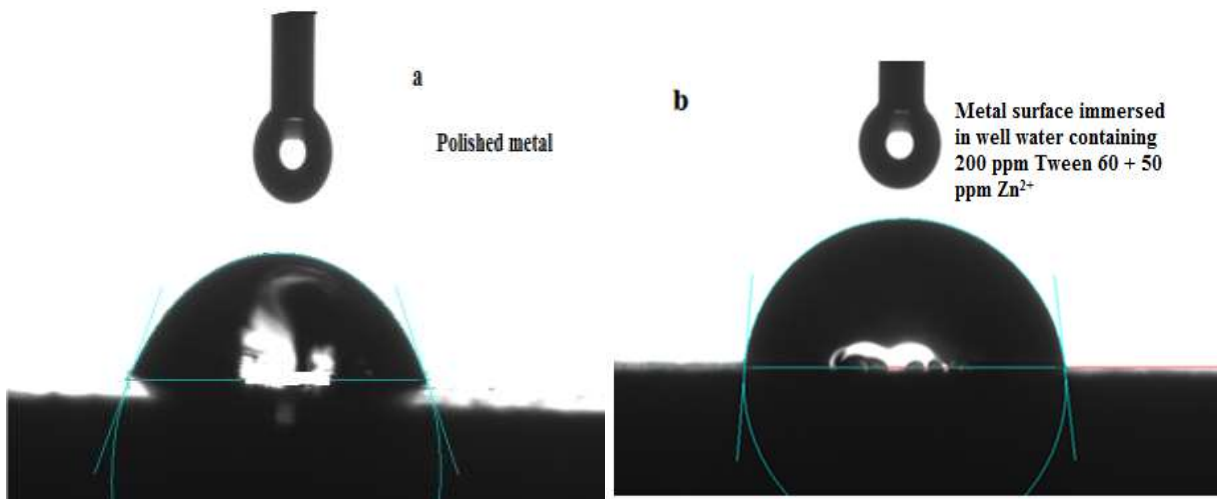


**Table 5. Contact angle measurement for polished metal and metal surface after immersion in well water containing 200 ppm of Tween 60 and 50 ppm of Zn<sup>2+</sup>.**

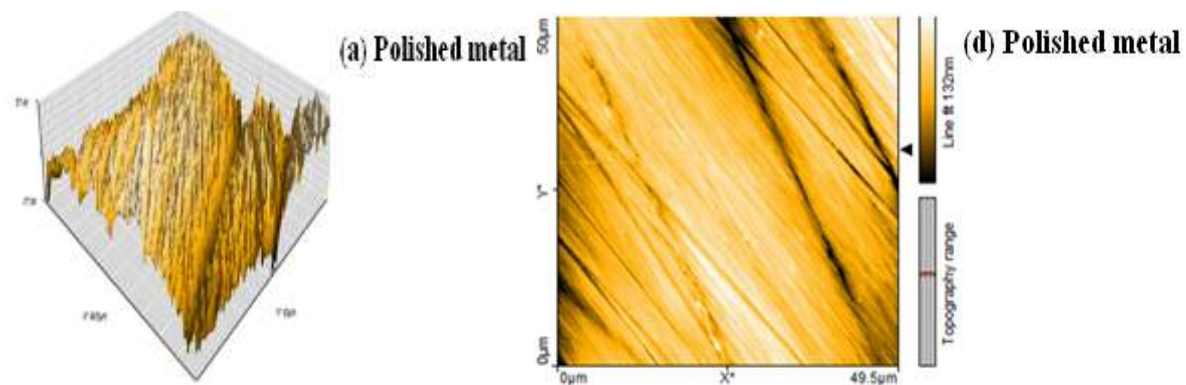
S.No	Contact angle value for polished metal	Contact angle value for metal surface after immersion in well water containing 200 ppm of Tween 60 and 50 ppm of Zn <sup>2+</sup>
1.	66°	84°

Contact angles of water droplets formed on various metal surfaces are given in the following Table 5. It is observed that for water droplet on polished mild steel surface the contact angle is 66°. In the case of metal surface immersed in the corrosion medium (well water) the contact angle increases to 84°. It is interest in note that in the presence of inhibitor, the contact angle increases by 18°.

Thus, it is evident that in presence of corrosion inhibitor (Tween 60), because of formation of Self-assembling nano films contact angle increases; hydrophobicity increases and hence corrosion inhibition increases Figures 6a and 6b.



**Figure 6. Contact angle measurement of (a) polished metal (b) Mild steel immersed in Well water (blank) + Tween 60 (200 ppm) + Zn<sup>2+</sup> (50 ppm)**



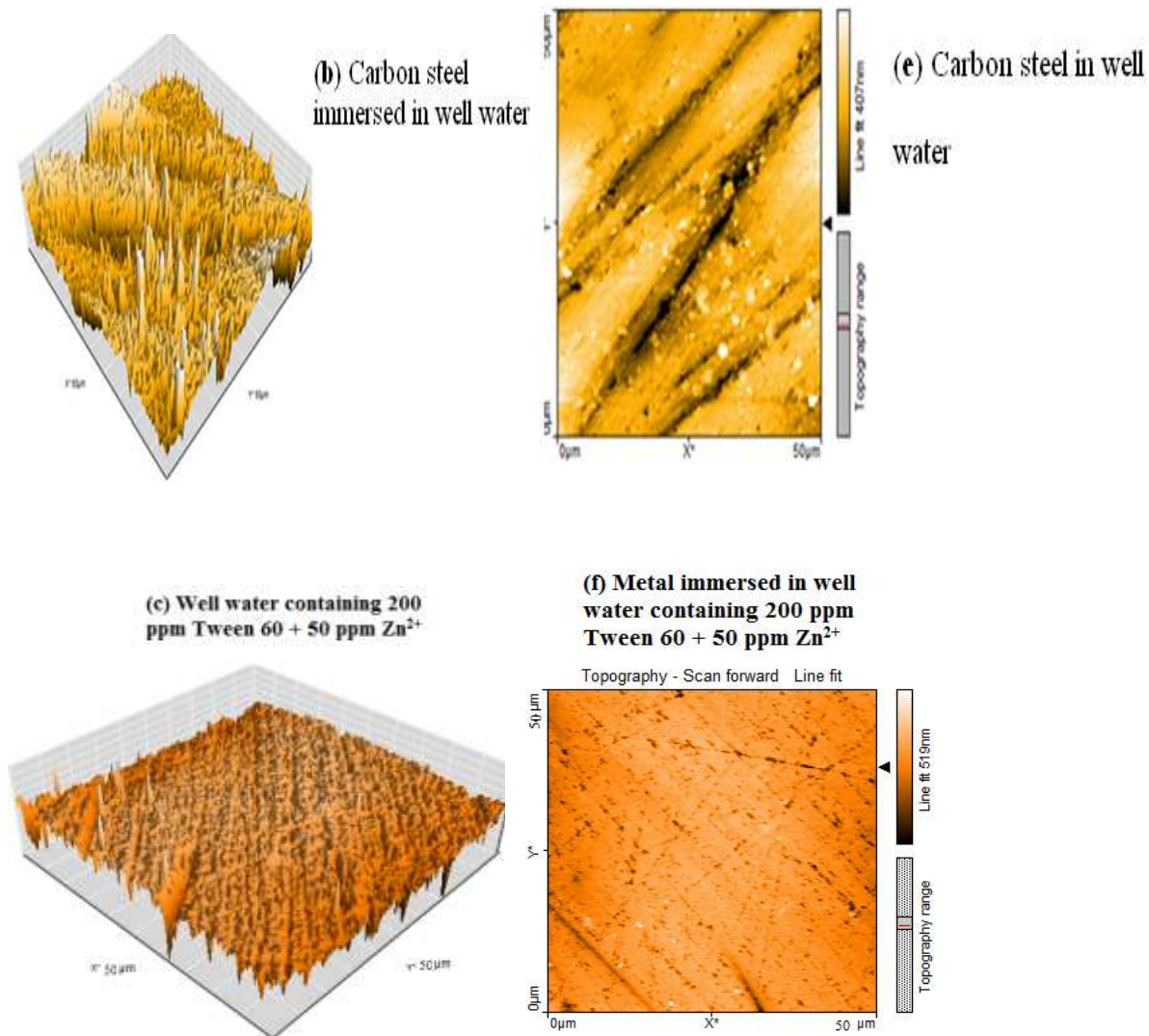


**Figure 7. Three dimensional AFM images of the surface of (a) polished mild steel (control) (b) Mild steel immersed in well water (blank) (c) Mild steel immersed in well water containing Tween 60 (200 ppm) +  $Zn^{2+}$  (50 ppm). Two dimensional AFM images of the surface of (d) Polished mild steel (control) (e) Mild steel immersed in well water (blank) (f) Mild steel immersed in well water containing Tween 60 (200 ppm) +  $Zn^{2+}$  (50 ppm).**

### Atomic force microscopy characterization

Atomic force microscopy is a powerful technique for gathering roughness statistics from a variety of surfaces<sup>21, 22, 23, 24</sup>. AFM is becoming an accepted method of roughness investigation. The two dimensional (2D), three dimensional (3D) of the AFM morphologies, AFM cross-sectional profile of surface for polished mild steel surface, mild steel surface immersed in well water and mild steel surface immersed in well water containing the formulation consisting of 200 ppm of Tween 60 and 50 ppm of  $Zn^{2+}$  are shown in Figures 7(a,b,c), (d,e,f) respectively.

### Root-mean-square roughness, average roughness, and peak-to-valley value

AFM image analysis was performed to get the average roughness,  $R_a$  (the average deviation of all points roughness profile from a mean line over the evaluation length), root-mean-square roughness,  $R_q$  (the average of the calculated height deviations taken within the evaluation length and measured from the mean line), and the maximum peak-to-valley (P-V) height values (largest single peak-to-valley height in five adjoining sampling heights). Table 6 is a summary of the average roughness ( $R_q$ ), RMS roughness ( $R_a$ ), maximum peak-to-valley height (P-V) values for mild steel surface immersed in different environments.

**Table 6. AFM data for mild steel immersed in inhibited and uninhibited environments.**

Sample	RMS ( $R_q$ ) roughness, nm	Average( $R_a$ ) roughness, nm	Maximum peak to valley height, nm
Polished mild steel (Control)	20.75	16.49	107.26
Mild steel immersed in well water (blank)	118.65	85.37	631.13
Mild steel immersed in well water containing Tween 60 (200 ppm) and $Zn^{2+}$ (50 ppm)s	46.56	39.07	219.01

The AFM images of mild steel immersed in well water in the absence and presence of  $Zn^{2+}$  are shown in Figures 7(a,b,c), (d,e,f). The values of ( $R_q$ ), ( $R_a$ ) and (P-V) height for the polished mild steel surface (Control) are 20.75 nm, 16.49 nm, and 107.26 nm, respectively. The small roughness observed on the polished mild steel surface is due to atmospheric corrosion. Figures 7 (b) and 7 (e) display the corroded metal surface with few pits in the absence of the inhibitor immersed in well water. The ( $R_q$ ), ( $R_a$ ), (P-V) height values for the mild steel surface are 118.65 nm, 84.37 nm and 631.13 nm, respectively. These data suggests that mild steel surface immersed in well water has a better surface roughness than the polished metal surface, which shows that the unprotected mild steel surface is rougher and was caused by the corrosion of the mild steel in the well water environment. Figures 7 (c) and 7 (f) display the steel surface after immersion in well water containing Tween 60 (200 ppm) +  $Zn^{2+}$  (50 ppm). The ( $R_q$ ), ( $R_a$ ), (P-V) height values for the mild steel surface are 46.56nm, 39.07 nm, and 219.01 nm, respectively. The ( $R_q$ ), ( $R_a$ ), (P-V) height values are considerably less in the inhibited environment compared to the uninhibited environment. These parameters prove that there is a formation of a protective film consisting of Self-assembling mono layers of Tween 60 and the surface is smoother. The smoothness of the surface is due to the development of Self-assembling mono layer of  $Fe^{2+}$ -Tween 60 complex and  $Zn(OH)_2$  on the metal surface, thereby inhibiting the corrosion of mild steel.

### Mechanism of Corrosion inhibition

The results of the weight-loss study show that the formulation consisting of 200 ppm of Tween 60 and 50 ppm of  $Zn^{2+}$  has 88 % IE in controlling corrosion of mild steel in well water. A synergistic effect exists between  $Zn^{2+}$  and Tween 60. Polarization study reveals that this formulation functions as mixed type inhibitor. AC impedance spectra reveal that a protective film (self-assembling nano film) is formed on the metal surface. FTIR spectra reveal that the protective film consists of  $Fe^{2+}$ - Tween 60 complex and  $Zn(OH)_2$ . Contact angle measurement reveal that the protective film is hydrophobic in nature. AFM data reveal that the protective film consisting of Self-assembling nano films of Tween 60on the metal surface. In order to explain these facts the following mechanism of corrosion inhibition is proposed.

- When the solution containing well water, 50 ppm  $Zn^{2+}$  and 200 ppm of Tween 60 is prepared, there is formulation of  $Zn^{2+}$ - Tween 60 complex in solution.
- When mild steel is immersed in this solution, the  $Zn^{2+}$ - Tween 60 complex diffuses from the bulk of the solution towards metal surface.
- $Zn^{2+}$ - Tween 60 complex diffuses from the bulk solution to the surface of the metal and is converted into a  $Fe^{2+}$ - Tween 60 complex, which is more stable than  $Zn^{2+}$ - Tween 60.
- On the metal surface  $Zn^{2+}$ - Tween 60complex is converted into  $Fe^{2+}$ - Tween 60 on the anodic sites,  $Zn^{2+}$  is released.  
 $Zn^{2+}$ - Tween 60 +  $Fe^{2+}$   $\rightarrow$   $Fe^{2+}$ - Tween 60 +  $Zn^{2+}$
- The released  $Zn^{2+}$  combines with  $OH^-$  to form  $Zn(OH)_2$  on the cathodic sites.  
 $Zn^{2+} + 2OH^- \rightarrow Zn(OH)_2 \downarrow$
- Thus the protective film consists of  $Fe^{2+}$ -Tween 60 complex and  $Zn(OH)_2$   $\downarrow$ .This accounts for the synergistic effect.
- FTIR spectra confirm that there is a formation of protective on the metal surface.
- Contact angle measurement confirm that the protective film is hydrophobic in nature.

- AFM images confirm that the protective film consisting of Self-assembling nanofilm of Tween 60 on the metal surface.

## Conclusions

- The present study leads to the following conclusions:
- The formulation consisting of 200 ppm of Tween 60 and 50 ppm of  $Zn^{2+}$  offers 88 % IE to mild steel immersed in aqueous solution
- A synergistic effect exists between Tween 60 and  $Zn^{2+}$
- Polarization study confirm that this formulation behaves as mixed inhibitor controlling both the anodic and cathodic reactions.
- AC impedance spectra and FTIR spectra confirm that a protective film is formed on the metal surface.
- Contact angle measurement confirm the hydrophobic nature of Self-assembling nano film of Tween 60.
- AFM data confirm that the Self-assembling nano film of Tween 60 is formed on the metal surface.

## Acknowledgement

The authors are thankful to their respective management for their help and encouragement.

## References

1. Fekry, A.M., and Mohamed, R.R., *ElectrochimicaActa*, 55 (6), 2010, 1933.
2. Yildiz, R., *Corrosion Science*, 90, 2015, 544.
3. Umoren, S.A., Obot, I.B., and Obi-Egbedi, N.O., *Journal of Materials Science*, 44, 2009, 274.
4. Singh, A.K., and Quraishi, M.A., *Corrosion Science*, 52, 2010, 152.
5. Abiola, O.K., and James, A.O., *Corrosion Science*, 52, 2010, 661.
6. Yamuna, J., and Noreen Anthony., *International Journal of MediPharm research*, 1(3), 2015, 184-192.
7. Ramya, K., and Muralimohan, N., *International Journal of Chemical Concepts*, 2(2), 2016, 70-75.
8. Yamuna, J., and Noreen Anthony., *International Journal of Technochem research*, 1(3), 2015, 175-182.
9. Fu, J.J., Li, S.N., Cao, L.H., Wang, Y., Yan, L.H., and Lu, L.D., *Journal of Materials Science*, 45, 2010, 979.
10. Zhang, D.Q., Cai, Q.R., Gao, L.X., and Lee, K.Y., *Corrosion Science*, 12, 2008, 3615.
11. Khaled, K.F., *Journal of Solid State Electrochemistry*, 13, 2009, 1743.
12. NazeeraBanu, V.R., Rajendran, S., and SenthilKumaran, S., *Journal of Alloys and Compounds*, 675,2016, 139-148. DOI: 10.1016/j.jallcom.2016.02.247
13. Noreen Antony,Benita Sherine, H., andSusaiRajendran, *PortugaliaeElectrochimicaActa*, 28(1), 2010, 1-14. DOI: 10.4152/pea.201001001
14. Fouda, A.S., Elewady, Y.A., Abd El-Aziz1, H.K., and Ahmed, A.M.,*International Journal of Electrochemical Science*, 7,2012,10456 – 10475.
15. I.A.Zaafarany, I.A.,*International Journal of Electrochemical Science*,8,2013,9531-9542.
16. Anbarasan, B., Rekha, S., Elango, K., Shriya, B., and Ramaprabhu, S., *International Journal of Pharmaceutical Sciences and Research*, 4(4), 2013, 1504-1513.
17. Ullah, S., Shariff, A.M., Bustam, M.A., Nadeem, M., Naz, M.Y., and Ayoub, M.,*International Journal of Electrochemical Science*,10,2015,9443 – 9455.
18. SusaiRajendran, Sribarathy, V., Nithyadevi, P., Angelin Thangakani, J., Robert Kennedy, Z., NazeeraBanu, N.,Satyabama, P., and Brindha, G.,*Elixir Nanotechnology*, 50, 2012, 10552-10555.
19. GregorZerjav, and Ingrid Milosev, *International Journal of Electrochemical Science*,9,2014,2696 – 2715.
20. Feroz Khan, Vaithianathan Shanthi, Rupesh K. Babu, Srinivasan Muralidharan, and Rakesh Chandra Barik,*Journal of Environmental Chemical Engineering*, 3, 2015, 10–19. DOI: 10.1016/j.jece.2014.11.005
21. Guannan Mu, and Xianghong Li, *Journal of Colloid and Interface Science*, 289, 2005, 184-192.DOI:10.1016/j.jcis.2005.03.061
22. Benita Sherine, Jamal Abdul Nasser, A., and Rajendran,S., *International journal of Engineering Science and Technology*, 2, 2010, 341-357.

23. Madhan, D., and Rajkumar, P., Der Pharma Chemica, 5 (5), 2013, 68-76.
24. Rajendran, S., Sribharathy, V., Krishnaveni, A., Sathiyabama, J., Robert Kennedy, Z., V.R.NazeeraBanu, V.R., and Brintha, G., Elixir Thin Film Technology, 2012, 50, 2012, 10509-10513.

\*\*\*\*\*